Distinct roles for precession, obliquity and eccentricity in 100kyr glacial cycles*

Stephen Barker[1**], Lorraine E. Lisiecki[2], Gregor Knorr[1,3], Sophie Nuber[1***], Polychronis C. Tzedakis[4]

1. School of Earth and Environmental Sciences, Cardiff University, UK
2. Department of Earth Science, University of California, Santa Barbara, USA
3. Alfred Wegener Institute for Polar Research, Bremerhaven, Germany
4. Environmental Change Research Centre, Department of Geography, University College London, UK

** Corresponding author barkers3@cf.ac.uk
*** Now at Department of Oceanography, University of Washington, USA

If accepted, the final version of this manuscript will be available via
doi: 10.1126/science.adp3491

Distinct roles for precession, obliquity and eccentricity in 100kyr glacial cycles

Stephen Barker[1*], Lorraine E. Lisiecki[2], Gregor Knorr[1,3], Sophie Nuber[1**], Polychronis C. Tzedakis[4]

1. School of Earth and Environmental Sciences, Cardiff University, UK
2. Department of Earth Science, University of California, Santa Barbara, USA
3. Alfred Wegener Institute for Polar Research, Bremerhaven, Germany
4. Environmental Change Research Centre, Department of Geography, University College London, UK

* Corresponding author barkers3@cf.ac.uk
** Now at Department of Oceanography, University of Washington, USA

Abstract

Attempts to discriminate between the specific roles of precession, obliquity and eccentricity in glacial/interglacial transitions have been hindered by imprecise age control. We circumvent this problem by focussing on the morphology of deglaciation/termination, which we show depends strongly on the relative phasing of precession versus obliquity. We demonstrate that while both parameters are important, precession has more influence on deglacial onset, while obliquity is more important for attainment of peak interglacial conditions and glacial inception. We find that the set of precession peaks responsible for terminations since 0.9Ma is a subset of those 'candidate peaks' which begin while obliquity is increasing. Specifically, termination occurs with the first candidate peak following a minimum in eccentricity. Thus the gross morphology of 100kyr glacial cycles appears largely deterministic.

1. Introduction

Following demonstration that the succession of Quaternary ice ages is fundamentally controlled by changes in Earth's orbital geometry (*1*) many studies have attempted to identify the precise roles of precession, obliquity and eccentricity in the waxing and waning of continental ice sheets, in particular the process of glacial termination (deglaciation). The main obstacles to such an exercise include the closeness in frequency of precession (~1/21kyr) to the 2nd harmonic of obliquity (~1/20.5kyr) and the dating precision required to demonstrate a clear and reproducible link between either parameter and the end of a glacial period. Consequently, there has been considerable debate as to whether precession (*2-5*), obliquity (*6, 7*) or some combination of the two (*8-11*) provides the dominant driving force for glacial termination and moreover as to why glacial terminations tend to be separated by ~100kyr (one of the main periods of eccentricity), hence the '100kyr problem' (*2, 12, 13*). Here we take an alternative approach, based on the assumption that if precession and obliquity play distinct roles in deglaciation, then variations in their relative phasing will be imprinted on the trajectory of ice volume change across individual terminations. Alternatively, if ice sheet variability depends only on (e.g.) the peak intensity of northern summer insolation at 65°N, then the relative phasing of precession and obliquity will leave no trace.

As with previous studies of this type (e.g. *2, 3, 5, 6, 10, 14*) we utilise the record of benthic foraminiferal $\delta^{18}O$ to infer changes in continental ice volume while acknowledging that the signal is impacted by variations in deep ocean temperature (*15, 16*). Indeed, a lead in the timing of mean ocean warming ahead of ice volume decrease across the most recent deglaciation (Termination 1, T1) (*17*) implies a difference of ~2kyr between the $\delta^{18}O$ signal recorded by benthic foraminifera and the component of $\delta^{18}O$ related specifically to ice volume (*18*). However, as we show below, this offset is relatively small compared to the variations in morphology observed (several kyr). Additionally, it has been suggested that the record of benthic $\delta^{18}O$ can be considered a proxy for Earth's energy imbalance across intervals of ice sheet

growth/decay and concomitant ocean cooling/warming (*18*). It could therefore be argued that the results reported here be interpreted in terms of the relative influences of precession and obliquity on Earth's energy imbalance associated with glacial/interglacial (G-IG) variability. We expand on this point within the supplementary material (*16*).

2. Quantifying deglacial morphology

We begin by quantifying the trajectory of benthic $\delta^{18}O$ across deglacial transitions and interglacials of the 100kyr world (approximately the last 800kyr; Figs. 1, 2). For this we use 3 independent stacks/records of benthic foraminiferal $\delta^{18}O$ (LR04/LR04_untuned (*14, 19*), HW04 (*20, 21*) and U1476pmag (*11*)) on 4 independent timescales (3 of which are free of orbital assumptions; See Methods (*16*)) to calculate the temporal offsets between 4 key points in the curve of $\delta^{18}O$ across each deglacial/interglacial period: (1) the onset of deglaciation (Onset deglac; when $\delta^{18}O$ begins to decrease following a glacial maximum (*16*)), (2) Max deglac: the point at which $\delta^{18}O$ reaches its maximum rate of decrease during termination, (3) Peak IG: the minimum in $\delta^{18}O$ associated with interglacial conditions and (4) Max inception: the subsequent maximum in the rate of $\delta^{18}O$ increase, marking a return to glacial conditions.

We do not define transitions between glacial and interglacial state based on a threshold in (e.g.) sea level or $\delta^{18}O$ (*10, 22*). Instead the points we select represent dynamical boundaries in the curve of $\delta^{18}O$ (e.g. Peak IG represents the change from decreasing to increasing $\delta^{18}O$ while Max deglac represents the maximum rate of deglaciation). As previously suggested (*23*) this approach has the advantage of providing logical points in the climate curve that we might expect to align with maxima (or minima) in forcing (e.g. we may expect that the maximum rate of ice loss during deglaciation should correspond to a maximum in the forcing responsible). We nevertheless think it is useful to adhere to common nomenclature (e.g. for describing glacial versus interglacial periods). We therefore follow the traditional marine isotope stratigraphic definition of an interglacial as a broad minimum in $\delta^{18}O$ bounded by sharp transitions to heavier values (*24*), which in this case are delineated by Max deglac and Max inception. By this definition an interglacial is divided into a period of deglaciation and a period of inception (Fig. 2A).

Our analysis suggests that variability in the total duration of deglaciation (from Onset deglac to Peak IG) is dominated by large (several kyr) changes in the offset between Max deglac and Peak IG (i.e. late deglaciation; Fig. 1C) while the offset between Onset deglac and Max deglac (early deglaciation) is comparatively constant (8.6±1kyr for LR04 or 8.9±0.4kyr if Termination T8 is excluded, 7.8±0.9kyr for HW04 and 10±1.7kyr for U1476pmag; Fig. S2F). The interval between Peak IG and Max inception (early inception) is also relatively invariant and is strongly correlated to the offset between Max deglac and Peak IG (R^2 = 0.96/0.99 for LR04/LR04_untuned, R^2 = 0.87 for HW04, R^2 = 0.73 for U1476pmag; Figs. 2B, S4). From these results it can be seen that the entire duration from Onset deglac through to Max inception might be predicted simply from the offset between Max deglac and Peak IG.

3. Orbital phasing determines the duration of deglaciation

Previously (*25*) it was suggested that the phasing between precession and obliquity influences the persistence of interglacial conditions. Our results (Fig. 1) suggest that variations in interglacial duration (from Max deglac to Max inception) are dominated by changes in the deglacial phase (i.e. between Max deglac and Peak IG). We might therefore expect to find a relationship between orbital phasing and the offset from Max deglac to Peak IG. To test for such a relationship we need to quantify the phasing between precession and obliquity at the time of each deglaciation. To this end we identify the nearest precession peak to each deglacial transition (i.e. closest to Max deglac) and calculate the offset between that peak and

its closest neighbouring peak in obliquity (Fig. 1D). Note that we use the term 'peak' (for both obliquity and precession) to describe conditions that give rise to a maximum in northern hemisphere summer insolation (which corresponds to a maximum in obliquity but a minimum in the precession parameter, when northern summer occurs during perihelion).

As stated, previous attempts to identify which orbital parameter might be more important for deglaciation have been limited by the requirement for accurate and precise age control of paleoproxy records. Our approach is much less sensitive to this requirement. Because we are looking for the closest precession peak to each deglaciation, the age models we employ are required only to have an accuracy of ~±10kyr (for comparison the stated uncertainties for LR04 and HW04 over the last 1Myr are ±4kyr and ±7kyr respectively). Accordingly the set of precession peaks identified for the last 11 terminations within LR04 is exactly the same for all of the records/timescales analysed here (Fig. S2), giving us confidence in the robustness of our selection criteria.

The analysis reveals a strong correlation between Max deglac minus Peak IG and the phasing of precession versus obliquity (Figs. 2C, 2D, S3) with R^2 ranging from 0.74 to 0.88 for the various records and age models employed. Note that the alternative approach, of identifying the closest obliquity peak to Max deglac and its nearest neighbouring precession peak would give an equivalent result but with a negative slope (*16*) (Fig. S5). The observation of such a strong imprint of the phasing between obliquity and precession on the evolution of $\delta^{18}O$ across deglaciation implies not only that both parameters play a role, but that these roles are somehow discrete (distinct), and therefore distinguishable.

4. Discrete roles for precession and obliquity in deglaciation and glacial inception

Recent studies aimed at providing more precise constraints on the timing of deglaciation have reached different conclusions about the relative importance of obliquity versus precession for the onset of deglaciation (*5, 7*). Our results (Fig. 2) suggest that the duration from Max deglac through to Max inception is a linear function of the offset between peak precession and peak obliquity at the time of deglaciation. Logically this implies that one parameter plays a more important role in the earlier stages of deglaciation (up to an including Max deglac) while the other is more influential on the latter stages and ultimately the subsequent glacial inception. To evaluate these possibilities we alternately force Max deglac to align with the peak in precession (obliquity) closest to each termination and assess the implied alignment of Peak IG and Max inception with respect to obliquity (precession). We expect this alignment to be stronger when the correct starting parameter is selected. Our choice to set Max deglac to align with a peak in either parameter follows the logic that the maximum rate in ice volume decrease should coincide approximately with a maximum in forcing (*23*). On the other hand the exact phase employed is not critical for the arguments that follow, only that the phase is consistent for each termination.

In Scenario I (the actual observations) we calculate the phase of precession and obliquity associated with each key point (Onset deglac, Max deglac, Peak IG and Max inception) in each record of benthic $\delta^{18}O$ over the last 1Myr based on their published age models (i.e. making no assumptions about which transition should align with what phase of which parameter). This interval includes 11 glacial terminations, but we exclude T1 because it has no subsequent inception. In Figure 3 (and Fig. S6) we show results only for the three age models that are independent of orbital assumptions (results including LR04 are given in Table S2). Results for Scenario I reveal a broad scatter of Max deglac around peaks in both obliquity and precession (Fig. S6A3, B3), suggesting (in keeping with previous studies (*5, 7, 8*)) that both parameters probably play some role in deglaciation. On the other hand obliquity alone seems to influence glacial inception, which is associated with decreasing to low obliquity (again consistent with previous work (*11, 25*)).

In Scenario II we set Max deglac to align with peak precession (Figs. 3A2, S6C3). We exploit the relationships shown in Figures 2, S3, S4 to predict the temporal offsets between Max deglac and Peak IG (and Max inception) for each deglaciation based on the observed orbital phasing in each case, and then calculate the phase of each event relative to the peak in precession or obliquity closest to Max deglac (Methods; *16*). We do the same for Onset deglac to Max deglac but using the measured offsets shown in Figure S2F. The results highlight a strong alignment of Onset deglac with respect to precession (mean resultant vector length, r = 0.87, see Methods (*16*); Figs. 3A2, S6C2). This is not surprising given that the offset between Onset deglac and Max deglac is relatively constant (e.g. Fig.1C), but it is notable that the average offset (8.5±1.7kyr before the peak in precession) is just less than half a precession cycle, implying that if Max deglac coincides with peak precession then the onset of deglaciation occurs ~2kyr after northern summer insolation begins to intensify (as a function of precession). In this scenario Onset deglac and Max deglac also align with increasing to high values of obliquity (Figs. 3B2, S6D2,3). In fact we observe stronger alignment in these cases than observed in Scenario I (r = 0.52 vs 0.46 and r = 0.54 vs 0.44 respectively; Table S2). Thus for Scenario II the onset of deglaciation occurs when northern summer insolation is increasing as a function of both precession and obliquity (implying a dual role for obliquity and precession in the process of deglaciation).

The most outstanding result from Scenario II is the very strong alignment of Peak IG with decreasing obliquity (very close to the maximum rate of decrease) and of Max inception with low to minimum obliquity (Figs. 3B2, S6D4,5). In each case we obtain r values in excess of 0.95, much higher than those obtained in Scenario I (although the phase relationships observed are similar; Table S2). In other words, when Max deglac is set to peak precession, Peak IG and Max inception align precisely with respect to obliquity. A version of Scenario II using the measured offsets from Max deglac to Peak IG and Max inception (rather than predicted) also gives r values greater than observed in Scenario I (r = 0.82 vs 0.64 and r = 0.72 vs 0.57 respectively; Table S2). The relationships between Peak IG and Max inception versus precession in Scenario II are not significant.

In Scenario III we set Max deglac to peak obliquity (Figs. 3B3, S6F3). We observe a strong alignment of Onset deglac with increasing obliquity (Fig. S6F2), analogous to Onset deglac versus precession in Scenario II. However, the relationships between Peak IG and Max inception versus precession are weak (r < 0.4) and although statistically significant for the combined records, this is not the case for any record when treated individually (Table S2). Notably in Scenario III, the relationships between Onset deglac and Max deglac versus precession are significantly worse than in Scenario I (Figs. 3A3, S6E2,3; Table S2) and imply that deglaciation is essentially independent of this parameter (i.e. no dual role for obliquity and precession in the process of deglaciation).

In summary, the results for Scenario II (in which Max deglac is aligned with peak precession) are consistent with a dual role for precession and obliquity in deglaciation and the proposition that precession plays a more important role in the precise timing of deglacial onset (*5*), while obliquity is more important for the timing of Peak IG and Max inception. The equivalent is not true for Scenario III. Setting Max deglac to peak obliquity does not result in strong alignment of Max inception with respect to precession and implies that no relationship exists between precession and deglaciation.

5. Importance of latitude and inadequacy of a single insolation metric

The combined effects of obliquity and precession (as modulated by eccentricity) on insolation are typically quantified using a single metric for example June 21 (peak summer) intensity or some measure of integrated summer insolation at 65°N. However, the relative contribution of obliquity versus precession to any given insolation metric decreases significantly as one moves from higher to lower latitudes (*11*) (Fig.

4A). Consequently, use of a single metric at a fixed latitude may be inadequate for defining the forcing relevant to an ice sheet whose mean latitude varies with time. Our results underscore this issue because they require that the relative importance of obliquity versus precession varies throughout a glacial cycle. Specifically, while precession appears to be more important for melting back very large ice sheets from their maximum extent, obliquity is more important for the end of glacial retreat and the beginning of the next glacial cycle. Glacial inception must occur at high latitude sites (north of ~70°N) such as the Canadian Arctic Archipelago (*26*). In these regions the contribution of obliquity to calorific summer insolation significantly outweighs that of precession (Fig. 4A). As ice sheets develop, their mean latitude will migrate southwards, to latitudes where precession is more important, until they attain their full glacial maximum position. At this point (anywhere south of ~55°N) precession dominates variations in both peak summer intensity and calorific summer insolation, which can explain why the early stages of deglaciation are more strongly dependent on this parameter. Thereafter, as ice sheets decay, they retreat back toward higher latitudes where obliquity dominates (Fig. 4A).

So far, we have not considered the absolute magnitude of insolation forcing necessary for producing significant changes in ice sheet size. For example, the magnitude of precession forcing associated with T5 (leading to MIS 11) was small (a consequence of reduced eccentricity; Fig. 4B). And yet the magnitude of ice volume change across T5 was greater than terminations which experienced much larger variations in precession; hence, the 'Stage 11 problem' (*12, 27*). On the other hand, the vulnerability of very large ice sheets to even modest variations in precession (*28*) might simply reflect their more southerly position (Fig. 4B). In addition, feedbacks within the climate system play an important role in amplifying orbital forcing (*29, 30*) and may therefore help to even out amplitude variations. For example, millennial-scale oscillations in ocean circulation and concomitant release of CO_2 during the early stages of termination can contribute to global warming at these times (*17, 31*), while equivalent activity during glacial development may actually help to cool the deep ocean and provide additional storage capacity for lowering atmospheric CO_2 (*16, 30, 32*) (an essential aspect of glacial inception (*33*)).

6. Precession, obliquity and eccentricity combine to produce ~100kyr glacial cycles

The dominant ~100kyr period of mid/late Pleistocene G-IG cyclicity (*1*) is problematic because direct orbital forcing at this period (via eccentricity) is weak (*12*). Most recent studies have concluded that the large magnitude of glacial terminations must involve forcing by some combination of precession and/or obliquity with additional feedbacks internal to the climate system (*29*) and our results shed light on how these parameters combine to produce the observed morphology of deglacial/interglacial periods. However, there remains the question as to why glacial cycles should endure for so long and why they have such a strong link to eccentricity (*14*) (Fig. 4B). Raymo (*2*) suggested that an extended interval of low amplitude precession forcing (under the influence of low eccentricity) would allow the build-up of large continental ice sheets by enabling them to expand southwards until they reached some critical size, after which they would become susceptible to even modest insolation forcing. Accordingly, most successful models of G-IG variability (*8, 9, 13, 34*) incorporate a critical ice volume threshold (V_{crit}), beyond which termination becomes possible/inevitable.

Our results provide empirical constraints for predicting the occurrence and duration of glacial terminations and interglacials since the Mid Pleistocene Transition (MPT i.e. the 100kyr world; Fig. 5) (*16*). As stated, the set of precession peaks associated with Max deglac for each termination of the past 1Myr is identical for all of the $\delta^{18}O$ records analysed here (Fig. S2). Furthermore, each of those peaks was aligned with average to high values of obliquity (Fig. 1D, E), which implies that obliquity was rising as peak summer intensity began increasing as a function of precession (*16*) (see orange symbols in Fig. 1D, E). Thus the onset of deglaciation occurred only when summers were warming through the reinforcing (dual) effects of obliquity and

precession (see also results in Fig. 3). In Figure 5H we plot all such 'candidate' precession peaks of the past 1Myr (i.e. those that began while obliquity was increasing or had started to increase within 2kyr of the turning point in precession; see Methods (*16*)).

Significantly the subset of candidate precession peaks resulting in termination over the past 900kyr were precisely those that directly followed a minimum in eccentricity (See Methods (*16*); Fig. 5H). That is, glacial termination occurred with the first candidate precession peak following each minimum in eccentricity (resulting in glacial cycles spanning 4 or 5 precession peaks with an average duration of ~95kyr (*16*)). This might suggest that V_{crit} is attained as soon as eccentricity reaches its minimum, after which the next candidate peak in precession triggers deglaciation. However, we note that in many cases, one or more non-candidate precession peaks occurred within the interval between the minimum in eccentricity and the terminating precession peak. Since non-candidate precession peaks are (by definition) those that align with low obliquity, continued ice growth during these intervals might also be critical for attainment of V_{crit} prior to termination (*13*). In any case, our observations allow us to construct an algorithm capable of predicting the occurrence of all major glacial terminations over the past 900kyr, based simply on the subset of candidate precession peaks that follow directly after minima in eccentricity (Fig. 5H). In Figure 5D we also incorporate predictions for the key points (Peak IG and Max inception), based on the phasing of precession versus obliquity during termination (Methods; *16*).

The results compare well with those obtained from a simple thresholding approach used to predict interglacials of the past 1Myr (*10*) (Fig. 5I), with 3 exceptions: (1,2) Our algorithm does not predict terminations T3a (into MIS 7c) or T7a (MIS 15a). While these events were aligned with candidate peaks (Fig. 5), they were relatively short in duration with respect to the phasing of precession versus obliquity (Fig. 2C, D) and do not fall within the set of major terminations. Notably though, they occurred when the amplitude of precession forcing was particularly large (thanks to high eccentricity). We therefore consider MIS 7c and 15a as anomalously warm substages, analogous to MIS 5a and 9a (Fig 5G) but of larger amplitude thanks to the direct influence of eccentricity on precession. (3) T6 was a protracted (2-step) termination (*35*), resulting in the delayed attainment of full interglacial conditions (MIS 13a) according to the prediction of (*10*). The preceding glacial (MIS 14) was particularly weak (*36*) and the smaller size of ice sheets (Fig. 5G) might explain the weaker response to orbital forcing associated with the first step (T6). The second step (T6a) was also aligned with a candidate precession peak and its duration (relative to orbital phasing) was in line with all other major terminations (Fig. 2C, D). Thus the full deglaciation from MIS 14 into MIS 13a could be considered as 2 distinct deglacial events, each following the pattern of other major terminations of the past 900kyr.

Our results suggest that the succession and duration of deglacial/interglacial events since the MPT might be largely determined by the relative phasing of precession, obliquity and eccentricity (Fig. 5D). This deterministic quality (previously inferred from theoretical/model-based approaches (*9, 37*)) provides an opportunity to hypothesise about the possible future of Earth's climate. There has been considerable discussion as to when the next glacial inception might occur (*33, 38-40*). Most studies agree that inception results from some critical combination of orbital configuration and the atmospheric concentration of CO_2 (*16*) and there is little debate that while CO_2 levels continue to rise there is almost no chance of a return to glacial conditions (*33, 40*). Notwithstanding, it is important to understand the natural variability of climate and how this might play out if and when the anthropogenic input of CO_2 is reduced to pre-industrial levels. We therefore calculate when the next glacial inception might occur (ignoring the effects of anthropogenic CO_2) based on the phasing of precession versus obliquity during the last deglaciation (T1) (*16*). We obtain an age of -0.1±1.8kyr (2σ) for MIS 1 Peak IG and -7.7±3.4kyr (2σ) for the next Max inception (Fig. S7D). Thus we estimate that, if not for the effects of increasing CO_2, glacial inception would reach a maximum rate within the next 11kyr. Our extrapolation also suggests that the next interglacial event would begin ~66kyr from now (following a glacial cycle spanning 4 precession peaks; Fig. 5D). On the other hand, while

atmospheric CO_2 remains above pre-industrial levels it is unlikely that glacial inception will occur (*33, 41*), in which case the pattern of future interglacials will be very different from the prediction made here.

Acknowledgements

We thank M. Crucifix for assistance with palinsol. This is Cardiff EARTH CRediT contribution 26.

References

1. J. D. Hays, J. Imbrie, N. J. Shackleton, Variations in the Earth's orbit: Pacemaker of the Ice Ages. *Science* **194**, 1121-1132 (1976).
2. M. E. Raymo, The timing of major climate terminations. *Paleoceanography* **12**, 577-585 (1997).
3. A. J. Ridgwell, A. J. Watson, M. E. Raymo, Is the spectral signature of the 100 kyr glacial cycle consistent with a Milankovitch origin? *Paleoceanography* **14**, 437-440 (1999).
4. H. Cheng, R. L. Edwards, A. Sinha, C. Spötl, L. Yi, S. Chen, M. Kelly, G. Kathayat, X. Wang, X. Li, The Asian monsoon over the past 640,000 years and ice age terminations. *Nature* **534**, 640-646 (2016).
5. B. Hobart, L. E. Lisiecki, D. Rand, T. Lee, C. E. Lawrence, Late Pleistocene 100-kyr glacial cycles paced by precession forcing of summer insolation. *Nature Geoscience* **16**, 717-722 (2023).
6. P. Huybers, C. Wunsch, Obliquity pacing of the late Pleistocene glacial terminations. *Nature* **434**, 491-494 (2005).
7. P. Bajo, R. N. Drysdale, J. D. Woodhead, J. C. Hellstrom, D. Hodell, P. Ferretti, A. H. Voelker, G. Zanchetta, T. Rodrigues, E. Wolff, Persistent influence of obliquity on ice age terminations since the Middle Pleistocene transition. *Science* **367**, 1235-1239 (2020).
8. P. Huybers, Combined obliquity and precession pacing of late Pleistocene deglaciations. *Nature* **480**, 229-232 (2011).
9. F. Parrenin, D. Paillard, Terminations VI and VIII (∼ 530 and∼ 720 kyr BP) tell us the importance of obliquity and precession in the triggering of deglaciations. *Climate of the Past* **8**, 2031-2037 (2012).
10. P. C. Tzedakis, M. Crucifix, T. Mitsui, E. W. Wolff, A simple rule to determine which insolation cycles lead to interglacials. *Nature* **542**, 427-432 (2017).
11. S. Barker, A. Starr, J. v. d. Lubbe, A. Doughty, G. Knorr, S. Conn, S. Lordsmith, L. Owen, A. Nederbragt, S. Hemming, I. Hall, L. Levay, Persistent influence of precession on northern ice sheet variability since the early Pleistocene. *Science* **376**, 961-967 (2022) doi: 10.1126/science.abm4033.
12. J. Imbrie, A. Berger, E. A. Boyle, S. C. Clemens, A. Duffy, W. R. Howard, G. Kukla, J. Kutzbach, D. G. Martinson, A. McIntyre, A. C. Mix, B. Molfino, J. J. Morley, L. C. Peterson, N. G. Pisias, W. L. Prell, M. E. Raymo, N. J. Shackleton, J. R. Toggweiler, On the structure and origin of major glaciation cycles 2. the 100,000-year cycle. *Paleoceanography* **8**, 699-735 (1993).
13. A. Ganopolski, Toward generalized Milankovitch theory (GMT). *Climate of the Past* **20**, 151-185 (2024).
14. L. E. Lisiecki, Links between eccentricity forcing and the 100,000-year glacial cycle. *Nature geoscience* **3**, 349-352 (2010).
15. H. Elderfield, P. Ferretti, M. Greaves, S. Crowhurst, I. N. McCave, D. Hodell, A. M. Piotrowski, Evolution of Ocean Temperature and Ice Volume Through the Mid-Pleistocene Climate Transition. *Science* **337**, 704-709 (2012).
16. See Supplementary Materials.
17. D. Baggenstos, M. Häberli, J. Schmitt, S. A. Shackleton, B. Birner, J. P. Severinghaus, T. Kellerhals, H. Fischer, Earth's radiative imbalance from the Last Glacial Maximum to the present. *Proceedings of the National Academy of Sciences* **116**, 14881-14886 (2019).
18. S. Shackleton, A. Seltzer, D. Baggenstos, L. E. Lisiecki, Benthic δ18O records Earth's energy imbalance. *Nature Geoscience* **16**, 797-802 (2023).
19. L. E. Lisiecki, M. E. Raymo, A Pliocene-Pleistocene stack of 57 globally distributed benthic $\delta^{18}O$ records. *Paleoceanography* **20**, DOI:10.1029/2004PA001071 (2005).

20. P. Huybers, C. Wunsch, A depth-derived Pleistocene age model: Uncertainty estimates, sedimentation variability, and nonlinear climate change. *Paleoceanography* **19**, (2004).
21. P. Huybers, Glacial variability over the last two million years: an extended depth-derived agemodel, continuous obliquity pacing, and the Pleistocene progression. *Quaternary Science Reviews* **26**, 37-55 (2007).
22. PIGS_of_PAGES, Interglacials of the last 800,000 years. *Reviews of Geophysics* **54**, 162-219 (2016).
23. G. Roe, In defense of Milankovitch. *Geophysical Research Letters* **33**, (2006) 10.1029/2006GL027817.
24. N. J. Shackleton, N. D. Opdyke, Oxygen isotope and palaeomagnetic stratigraphy of Equatorial Pacific core V28-238: Oxygen isotope temperatures and ice volumes on a 105 year and 106 year scale. *Quaternary Research* **3**, 39-55 (1973).
25. P. C. Tzedakis, E. Wolff, L. Skinner, V. Brovkin, D. Hodell, J. F. McManus, D. Raynaud, Can we predict the duration of an interglacial? *Climate of the Past* **8**, 1473-1485 (2012).
26. P. Clark, J. Clague, B. B. Curry, A. Dreimanis, S. Hicock, G. Miller, G. Berger, N. Eyles, M. Lamothe, B. Miller, Initiation and development of the Laurentide and Cordilleran ice sheets following the last interglaciation. *Quaternary Science Reviews* **12**, 79-114 (1993).
27. P. C. Tzedakis, D. A. Hodell, C. Nehrbass-Ahles, T. Mitsui, E. W. Wolff, Marine isotope stage 11c: An unusual interglacial. *Quaternary Science Reviews* **284**, 107493 (2022).
28. A. Abe-Ouchi, F. Saito, K. Kawamura, M. E. Raymo, J. i. Okuno, K. Takahashi, H. Blatter, Insolation-driven 100,000-year glacial cycles and hysteresis of ice-sheet volume. *Nature* **500**, 190-193 (2013).
29. S. Barker, G. Knorr, Millennial scale feedbacks determine the shape and rapidity of glacial termination. *Nature Communications* **12**, 2273 (2021) 10.1038/s41467-021-22388-6.
30. S. Barker, G. Knorr, A Systematic Role for Extreme Ocean-Atmosphere Oscillations in the Development of Glacial Conditions Since the Mid Pleistocene Transition. *Paleoceanography and Paleoclimatology* **38**, e2023PA004690 (2023).
31. G. Knorr, S. Barker, X. Zhang, G. Lohmann, X. Gong, P. Gierz, C. Stepanek, L. B. Stap, A salty deep ocean as a prerequisite for glacial termination. *Nature Geoscience* **14**, 930-936 (2021).
32. S. Shackleton, J. A. Menking, E. Brook, C. Buizert, M. N. Dyonisius, V. V. Petrenko, D. Baggenstos, J. P. Severinghaus, Evolution of mean ocean temperature in Marine Isotope Stage 4. *Climate of the Past* **17**, 2273-2289 (2021).
33. A. Ganopolski, R. Winkelmann, H. J. Schellnhuber, Critical insolation–CO2 relation for diagnosing past and future glacial inception. *Nature* **529**, 200-203 (2016).
34. D. Paillard, The timing of Pleistocene glaciations from a simple multiple-state climate model. *Nature* **391**, 378 (1998).
35. S. Barker, G. Knorr, S. Conn, S. Lordsmith, D. Newman, D. Thornalley, Early interglacial legacy of deglacial climate instability. *Paleoceanography and Paleoclimatology*, (2019) 10.1029/2019PA003661.
36. N. Lang, E. W. Wolff, Interglacial and glacial variability from the last 800 ka in marine, ice and terrestrial archives. *Climate of the Past* **7**, 361 (2011).
37. M. Willeit, A. Ganopolski, R. Calov, V. Brovkin, Mid-Pleistocene transition in glacial cycles explained by declining CO2 and regolith removal. *Science Advances* **5**, eaav7337 (2019).
38. P. C. Tzedakis, J. Channell, D. Hodell, H. Kleiven, L. Skinner, Determining the natural length of the current interglacial. *Nature Geoscience* **5**, 138-141 (2012).
39. A. Berger, M. F. Loutre, An exceptionally long interglacial ahead? *Science* **297**, 1287-1288 (2002).
40. G. Vettoretti, W. Peltier, The impact of insolation, greenhouse gas forcing and ocean circulation changes on glacial inception. *The Holocene* **21**, 803-817 (2011).
41. D. Archer, A. Ganopolski, A movable trigger: Fossil fuel CO2 and the onset of the next glaciation. *Geochemistry Geophysics Geosystems* **6**, (2005).
42. A. Berger, M. F. Loutre, Insolation Values for the Climate of the Last 10 Million Years. *Quaternary Science Reviews* **10**, 297-317 (1991).
43. M. Crucifix, Palinsol: insolation for palaeoclimate studies, R package version 0.93. https://bitbucket.org/mcrucifix/insol (2016).
44. C. Waelbroeck, J. C. Duplessy, E. Michel, L. Labeyrie, D. Paillard, J. Duprat, The timing of the last deglaciation in North Atlantic climate records. *Nature* **412**, 724-727 (2001).

45. N. J. Shackleton, M. A. Hall, E. Vincent, Phase relationships between millennial-scale events 64,000-24,000 years ago. *Paleoceanography* **15**, 565-569 (2000).
46. R. B. Alley, E. J. Brook, S. Anandakrishnan, A northern lead in the orbital band: north-south phasing of Ice-Age events. *Quaternary Science Reviews* **21**, 431-441 (2002).
47. A. Schmittner, O. A. Saenko, A. J. Weaver, Coupling of the hemispheres in observations and simulations of glacial climate change. *Quaternary Science Reviews* **22**, 659-671 (2003).
48. S. Barker, G. Knorr, Antarctic climate signature in the Greenland ice core record. *Proceedings of the National Academy of Sciences of the United States of America* **104**, 17278-17282 (2007).
49. L. Skinner, N. Shackleton, Deconstructing Terminations I and II: revisiting the glacioeustatic paradigm based on deep-water temperature estimates. *Quaternary Science Reviews* **25**, 3312-3321 (2006).
50. G. H. Denton, R. F. Anderson, J. R. Toggweiler, R. L. Edwards, J. M. Schaefer, A. E. Putnam, The Last Glacial Termination. *Science* **328**, 1652-1656 (2010).
51. D. M. Sigman, M. P. Hain, G. H. Haug, The polar ocean and glacial cycles in atmospheric CO_2 concentration. *Nature* **466**, 47-55 (2010).
52. J. F. Adkins, The role of deep ocean circulation in setting glacial climates. *Paleoceanography* **28**, 539-561 (2013).
53. P. Berens, CircStat: a MATLAB toolbox for circular statistics. *J Stat Softw* **31**, 1-21 (2009).
54. J. V. Stern, L. E. Lisiecki, Termination 1 timing in radiocarbon-dated regional benthic δ18O stacks. *Paleoceanography* **29**, 1127-1142 (2014).
55. B. Bereiter, S. Shackleton, D. Baggenstos, K. Kawamura, J. Severinghaus, Mean global ocean temperatures during the last glacial transition. *Nature* **553**, 39 (2018).
56. K. Lambeck, H. Rouby, A. Purcell, Y. Sun, M. Sambridge, Sea level and global ice volumes from the Last Glacial Maximum to the Holocene. *Proceedings of the National Academy of Sciences* **111**, 15296-15303 (2014).

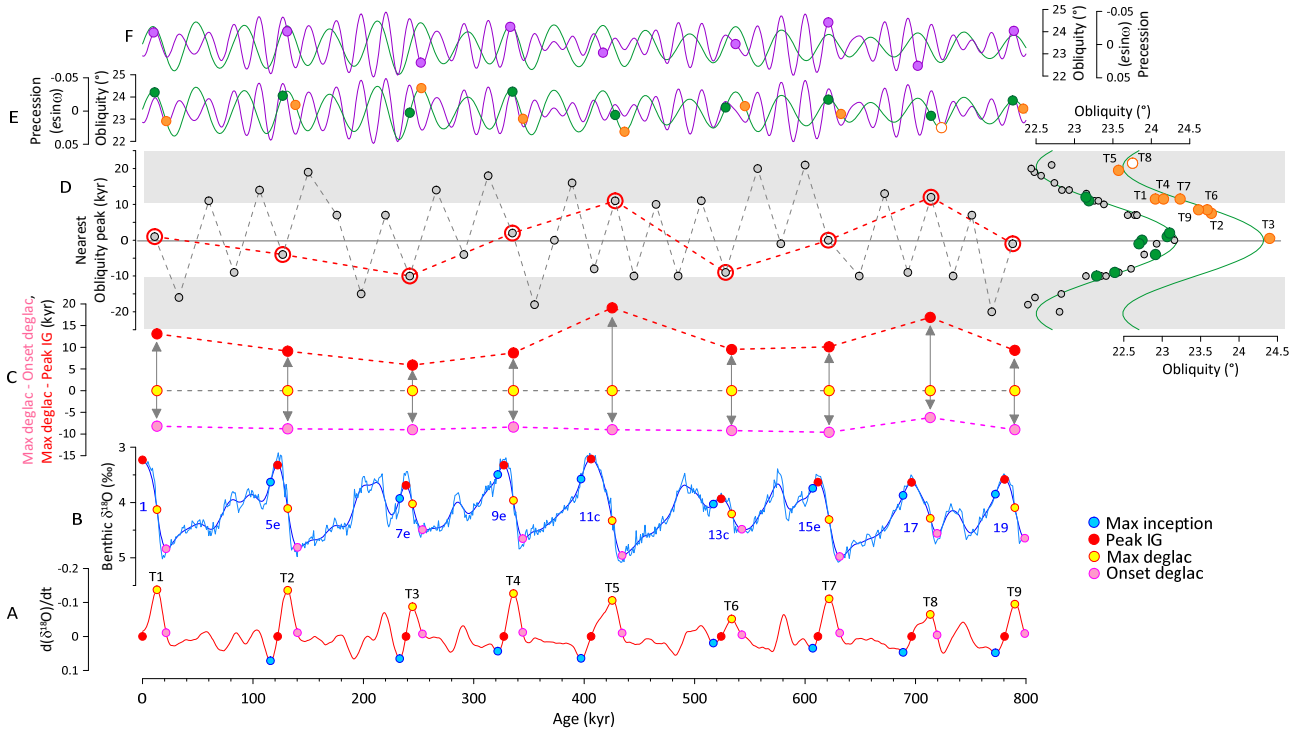

Figure 1 Deglacial morphology and the phasing of obliquity versus precession. (A, B) The LR04 benthic $\delta^{18}O$ stack (B) and its first derivative (A), used to identify the key points as described in main text (coloured symbols). Terminations are numbered T1-T9, MIS numbers in blue. (C) Calculated temporal offsets: Max deglac minus Onset deglac (pink symbols), Max deglac minus Peak IG (red). Variability in the duration of deglaciation (double-headed grey arrows) is dominated by changes in the offset between Max deglac and Peak IG. (D) Precession peaks plotted versus their temporal offset to the closest obliquity peak in each case. Large red symbols (joined by dashed lines) are those precession peaks that are closest to Max deglac in each case. All of these coincide with moderate to high values of obliquity as demonstrated by green symbols to right. Also plotted is the value of obliquity (orange symbols) associated with the beginning of each terminal precession peak (i.e. when the precession parameter shifts from increasing to decreasing; see also Part E and discussion in Section 6). (E) Precession and obliquity (*42*) over last 1Myr. Green symbols highlight value of obliquity at each terminal precession peak, orange symbols highlight phase of obliquity at the beginning of each terminal precession peak (increasing in all cases except T8, which starts to increase within 2kyr; see Methods (*16*)). (F) Same as E but purple symbols reflect value of precession parameter for the closest obliquity maximum to each Max deglaciation (no systematic pattern is observed cf. Fig. S6E3).

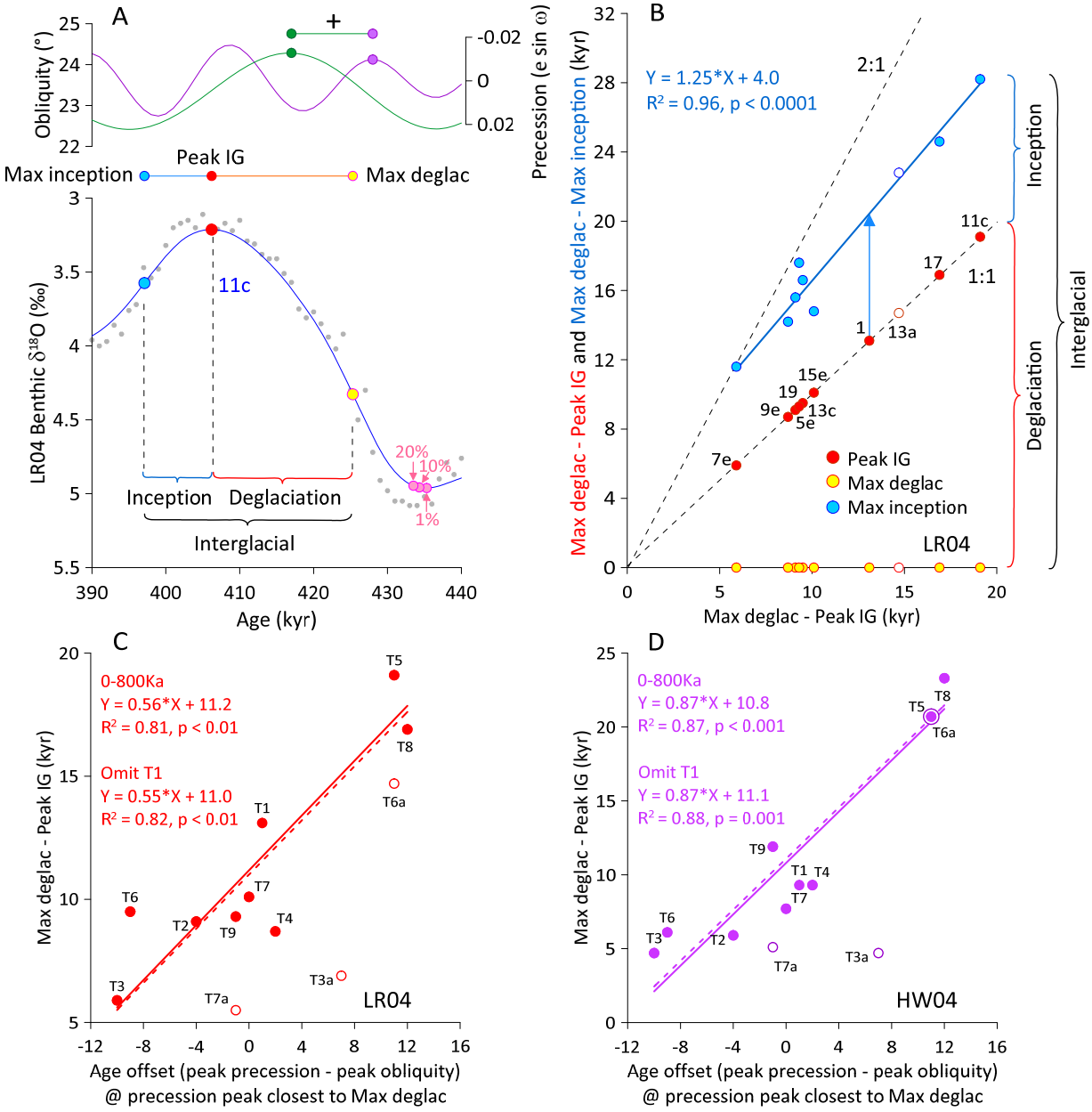

Figure 2 Orbital phasing determines the duration of deglaciation. (A) Detail of interglacial anatomy for MIS 11c (associated with T5). Each interglacial is divided into a period of deglaciation (between Max deglac and Peak IG) and inception (between Peak IG and Max inception). The pink symbols between 435-433ka indicate Onset deglaciation using 1, 10 and 20% of maximum rate of $\delta^{18}O$ decrease as threshold (see Methods). Upper curves of precession and obliquity highlight offset between their respective peaks (positive in this case). (B) Correlation between Max deglac minus Max inception and Max deglac minus Peak IG (numbers are MIS). The interval of inception is relatively invariant as compared with that of deglaciation, giving rise to increasingly asymmetric interglacials as their duration increases (see also Fig. S7A-C). The high value of R^2 implies that time to Max inception might be predicted for MIS 1 if we know the offset between Max deglac and Peak IG (blue arrow; see also Fig. S7D). (C, D) Correlation between Max deglac minus Peak IG and peak precession minus peak obliquity for LR04 and HW04. Dashed fits omit T1. Note that T3a, T6a/MIS13a and T7a (hollow symbols) are not included in the correlations (see discussion in Section 6). Equivalent correlations for other records are given in Figs. S3, S4.

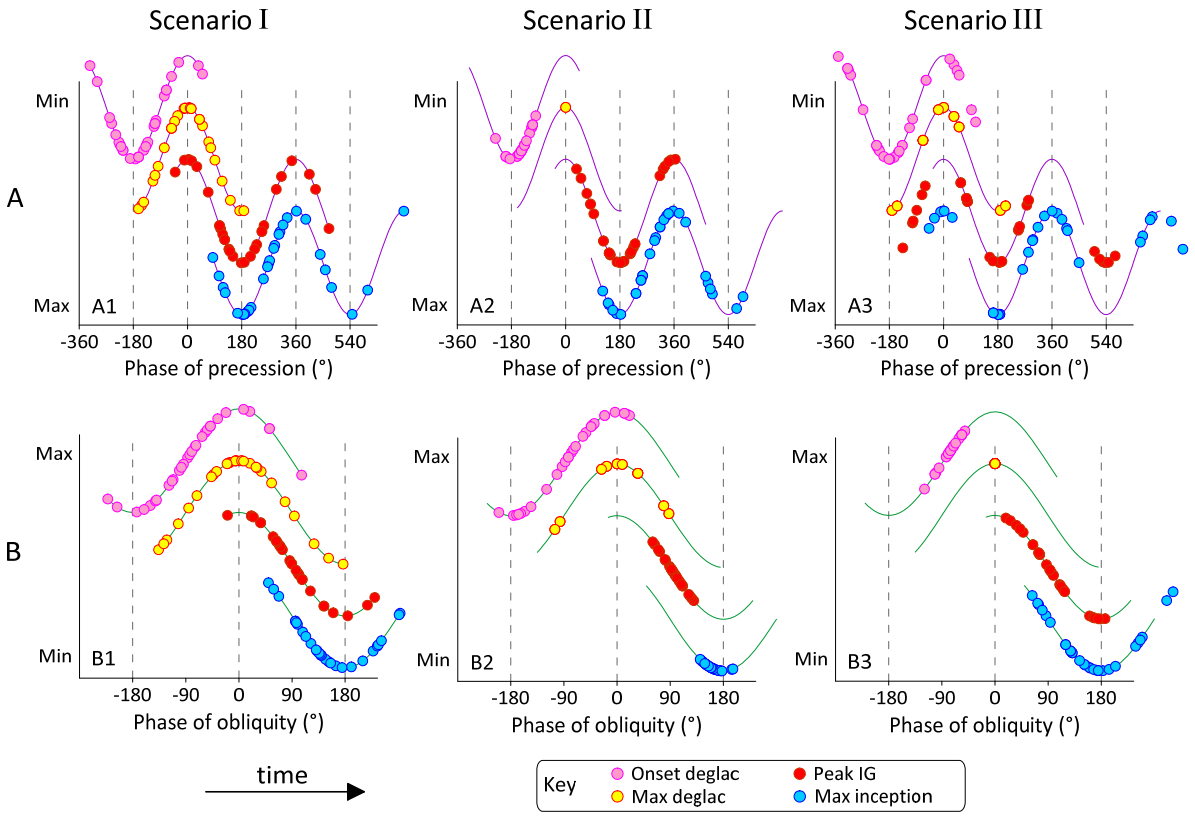

Figure 3 Inception aligns with obliquity when Max deglac is set to precession. Results for LR04_untuned, HW04 and U1476pmag from Scenarios I-III in Section 4. Each panel shows timing of Onset deglac, Max deglac, Peak IG and Max inception with respect to the phase of precession (row A) and obliquity (row B) for Terminations T2 to T12. In each case, zero phase is the closest precession/obliquity peak to Max deglac. Each individual point represents an individual termination/interglacial on one of the 3 timescales used. 10 terminations and 3 records gives a total of 30 points in each case (note some points are overlapping). Note in Scenario II (Max deglac set to peak precession; Part A2) much tighter clustering of Peak IG and Max inception with respect to obliquity (B2) as compared with Scenario I (B1). On the contrary, setting Max deglac to peak obliquity (Scenario III; B3) does not result in close alignment of Peak IG or Max inception with precession (A3). In addition, alignment between Onset deglac and Max deglac with respect to precession in Scenario III (A3) is significantly worse than in Scenario I (A1). See Figure S6 and Table S2 for more detail.

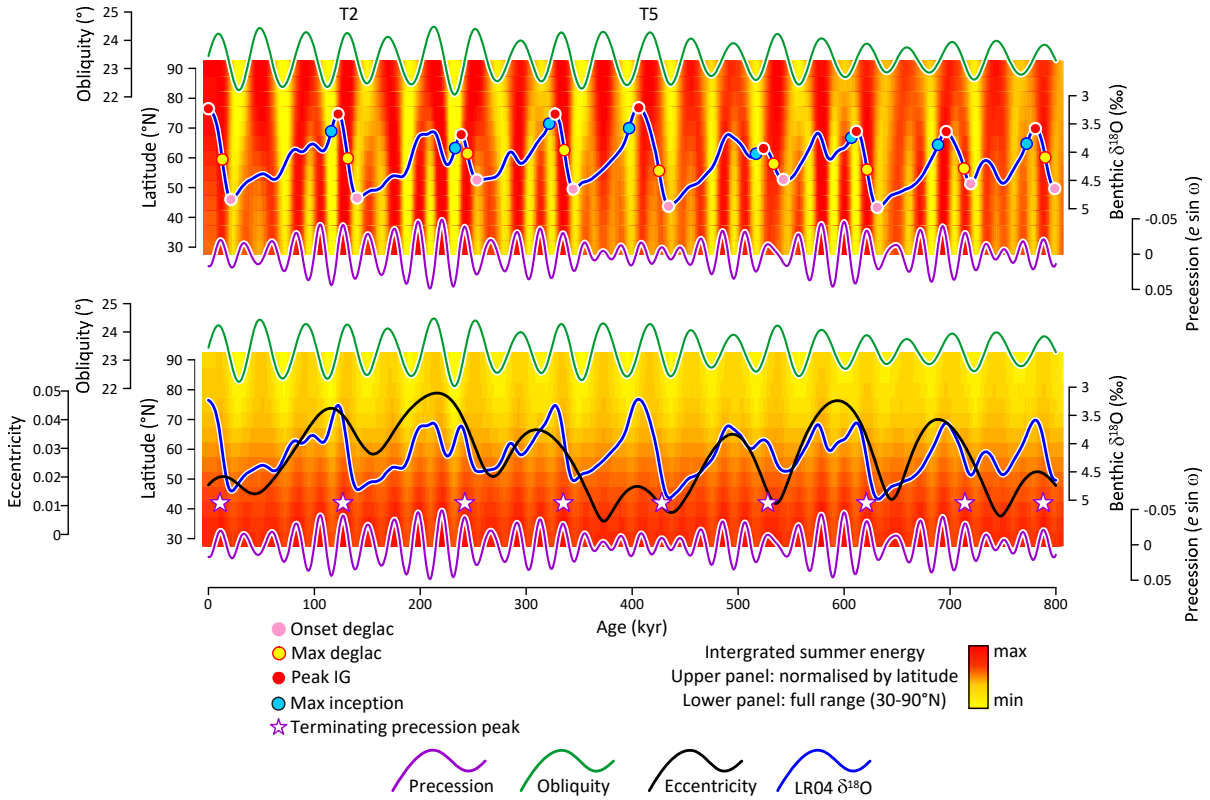

Figure 4 Importance of latitude and inadequacy of a single insolation metric. (Upper panel) Upper and lowermost curves are obliquity and precession respectively (*42*), middle blue curve is the smoothed LR04 stack (*19*). Key events are indicated. Orange/yellow colours represent the integrated summer energy (*43*) normalised by each 5 degree band of latitude. Variability at lower latitudes is dominated by precession while higher latitudes (north of around 70°N) are dominated by obliquity. If deglaciation reflects the northward migration of the mean latitude (locus) of northern hemisphere land-based ice sheets, it can be appreciated why precession (at low latitudes) is more important for the earlier stages of deglaciation, while obliquity (at high latitudes) is more important for the end. No single insolation metric can be used to characterise this changing dependence. Note that for T5 (~420ka) precession and obliquity were out of phase, giving rise to a particularly long deglacial period as the initial stages of deglaciation gave way to the subsequent (lagged) development of full interglacial conditions. In contrast precession and obliquity were in phase during T2 (~130ka), resulting in a much shorter interval of deglaciation. (Lower panel) Same as upper except that integrated summer energy is normalised across its entire range from 30 to 90°N. Ice sheets grow while eccentricity (black curve) decreases and obliquity is low. Purple stars are terminating precession peaks. Deglaciation may be triggered even if the amplitude of precession (a function of orbital eccentricity) is low (e.g. during T5) if ice sheets extend further to the south, where insolation is generally much higher than across more northerly latitudes.

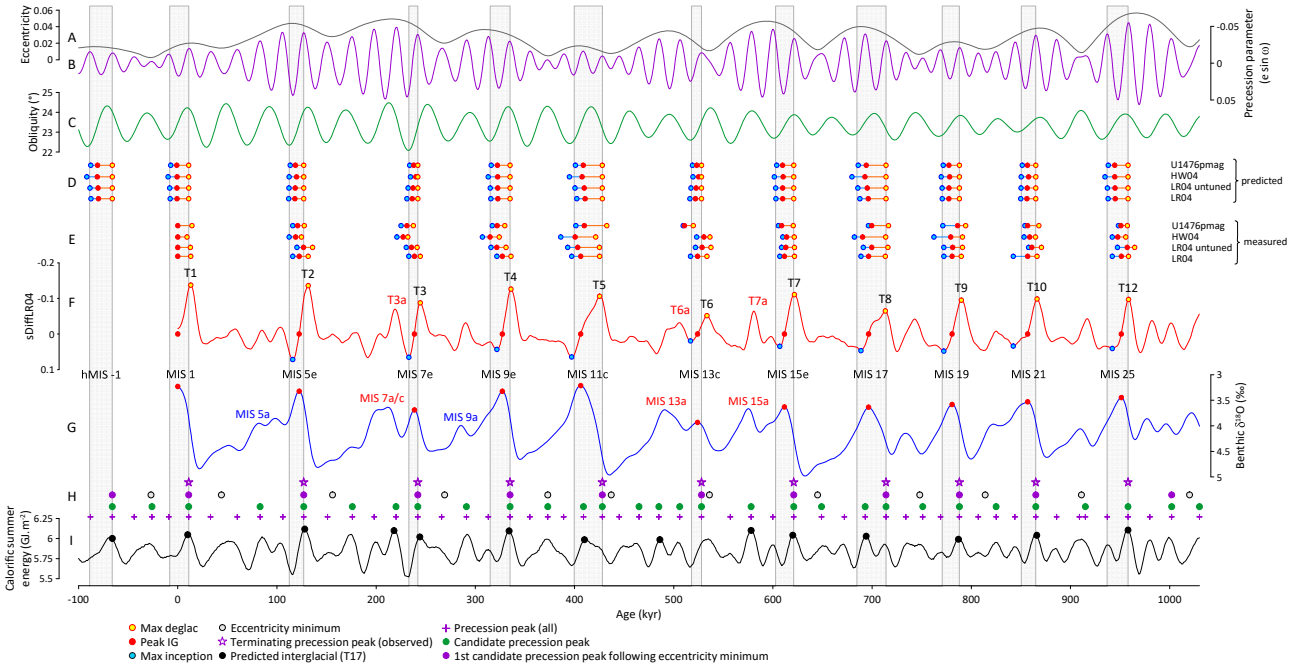

Figure 5 Predicted occurrence and duration of glacial terminations and interglacials. (A-C) precession, obliquity and eccentricity (*42, 43*). (D) key events (Max deglac, Peak IG and Max inception) predicted from the relationships shown in Figs. 2C,D, S3,4. (E) same events measured directly from records of $\delta^{18}O$. (F) first differential of the LR04 stack (G). (H) Terminating precession peaks of the last 900kyr (purple stars and solid purple circles) are the subset of candidate peaks (green circles), which directly follow minima in eccentricity (grey circles). Candidate peaks are the subset of precession peaks (purple crosses) which begin when obliquity is increasing (or starts to increase within 2kyr of the turning point in precession (*16*)). (I) Integrated summer energy at 65°N (*43*) with black symbols indicating the predicted occurrence of interglacials based on the rule of ref (*10*) (T17). hMIS-1 is a hypothetical future interglacial. Vertical grey boxes indicate the predicted duration of interglacial periods (from Max deglac to Max inception) based on the average of predicted events in part (D).